Proceedings 10th NUMGE 2023
10th European Conference on Numerical Methods in Geotechnical Engineering
Zdravkovic L, Kontoe S, Taborda DMG, Tsiampousi A (eds)

https://doi.org/10.53243/NUMGE2023-113

Investigations on a novel gravitational energy storage system using a high-cycle accumulation model

L. Mugele[1], A. Niemunis[1], A. Lamparter[1], H.H. Stutz[1]

[1]*Institute of Soil Mechanics and Rock Mechanics (IBF), Karlsruhe Institute of Technology, Karlsruhe, Germany*

ABSTRACT: One of the main concerns of our days is moving away from fossil fuels and implementing renewable energy sources into the energy supply. Large-scale energy storage is one of the biggest obstacles to the energy system's change. The required energy storage systems are not yet available. This paper presents a novel concept for gravitational energy storage. The energy storage is realised in the form of potential energy in the subsurface by injecting a pressurised fluid into a previously generated cavity. High pressures can be achieved in the inflatable cavity, allowing a large amount of energy to be stored. Numerical calculations of a deep cavity are presented. The boundary condition of the charging and discharging of the cavity are realised in the FEM simulation using a fluid link. The explicit high-cycle accumulation model is applied, whereby both the soil behaviour and the energy storage capacity can be evaluated. The preliminary results are promising in the aspect of energy efficiency and storage capacity of the proposed system.

Keywords: gravitational energy storage, high-cyclic loading, high-cycle accumulation model, hypoplasticity with intergranular strain

1 INTRODUCTION

The global energy transition is leading to a continuous increase in the installed capacity of renewable energies. This mainly applies to photovoltaics and wind energy which are affected by significant natural fluctuations. The need for energy storage capacity is continually increasing to store excess renewable energy and utilize it at a later time when the energy demand arises.

Currently, various options exist for storing surplus electrical energy. These include chemical, electrochemical, electrical, and thermal energy storage methods. However, the technology of pumped hydroelectric energy storage (PHES) systems is the most advanced technique (Blakers et al., 2021). The idea behind the PHES is to pump water up to a higher elevation using excess electrical energy and store that potential energy. Thereby, an efficiency of 80% can be reached (Blakers et al., 2021). However, this requires a suitable topography and a large area, which limits further expansion.

The novel concept known as an underground pumped hydroelectric storage system (UPHES) aims to store energy by lifting a mass of soil. A pressurised and impermeable (geomembrane-enveloped) cavity that can be charged or discharged with water is used to elevate the soil mass. The stored energy corresponds in a first approximation to the potential energy of the lifted soil mass (Olsen et al., 2015; Sørensen et al., 2021). The concept of a UPHES is shown in Figure 1.

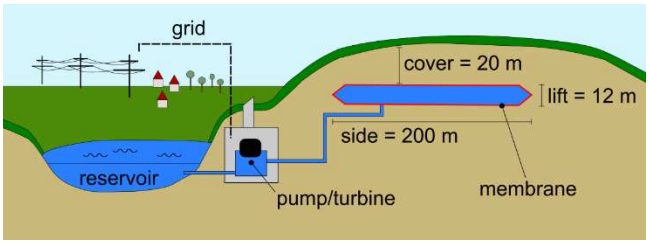

Figure 1. Concept of an underground pumped hydroelectric storage system (UPHES), modified from Sørensen (2021)

In previous studies, the presented system has already been investigated by conducting model experiments (Olsen et al., 2015; Sørensen et al., 2021), field tests (Franza et al., 2022; Olsen et al., 2015), centrifuge experiments (Franza et al., 2022) and numerical calculations taking into account advanced constitutive models, such as the hypoplastic model with intergranular strain (Norlyk et al., 2020; Stutz et al., 2020).

The UPHES is a highly promising and cost-effective system, particularly in coastal regions with high wind energy production potential. However, the system has several drawbacks such as significant energy losses and soil deformations, geomembrane failures, and accumulative effects. All of these effects have been observed in previous studies.

The essential modification of the novel UPHES, presented for the first time in this paper, is to increase the installing depth of the cavity significantly (up to 100 m). As a result of the increased pressure in the cavity, the same amount of energy can be stored with a reduced uplift per cycle, allowing for a lower volume amplitude.

The resulting strain amplitude in the soil is further reduced by a load distribution layer that balances the load above the cavity. These adjustments optimise the energy storage system, especially concerning the long-term performance of the whole system.

Considering these modifications the system is numerically investigated, using the high-cycle accumulation (HCA) model (Niemunis et al., 2005). As a result, the behaviour of the soil can be examined over the entire lifetime of 50 years (about $2 \cdot 10^4$ charges with one cycle of storage per day). Previous studies on the UPHES considered a smaller number of cycles due to the limitations of the constitutive model used (Norlyk et al., 2020; Stutz et al., 2020). This paper presents quasi-static FE calculations using the HCA model.

From the results, conclusions can be made regarding the long-term stability for both the geotechnical stability and the settlement behaviour in the overlying sand as well as energy storage capacity. The primary goal of this contribution is to investigate the cumulative soil behaviour as a result of the high-cycle loading caused by the energy storage system's intended application.

2 HIGH-CYCLE ACCUMULATION MODEL

Granular materials manifest a significant cumulative deformation behaviour due to cyclic deformation. Conventional, so-called implicit constitutive models are not adequate for an accurate simulation of the cumulative effects caused by high-cycle loading (Osinov, 2017). Most implicit models are not calibrated for high cyclic experiments.

The cumulative mechanical response of sand under high cyclic loading and small strain amplitudes ($\varepsilon^{\text{ampl}} < 10^{-3}$) can be numerically modeled using the barotropic, elasto-plastic, high cycle accumulation model (HCA) of Niemunis et al. (2005). This explicit constitutive model follows just the trend of accumulation as a function of the number of cycles. With the rate per cycle $d\,\sqcup/dN = \hat{\sqcup}$, the Equation (1) for the HCA model has the form

$$\hat{\boldsymbol{\sigma}} = \boldsymbol{E} : (\hat{\boldsymbol{\varepsilon}} - \hat{\boldsymbol{\varepsilon}}^{\text{acc}} - \hat{\boldsymbol{\varepsilon}}^{pl}) \qquad (1)$$

with the stress rate $\hat{\boldsymbol{\sigma}}$ of the effective Cauchy stress $\boldsymbol{\sigma}$, the strain rate $\hat{\boldsymbol{\varepsilon}}$ (the monotonic trend), the plastic strain rate $\hat{\boldsymbol{\varepsilon}}^{pl}$ and the accumulated strain rate $\hat{\boldsymbol{\varepsilon}}^{\text{acc}}$. $\mathbf{E}$ is a barotropic elastic stiffness and the accumulation rate $\hat{\boldsymbol{\varepsilon}}^{\text{acc}}$ is described by the flow rule (unit tensor) $\boldsymbol{m}$, which is determined by the current stress state, and the scalar accumulation intensity $\hat{\varepsilon}^{acc}$:

$$\hat{\boldsymbol{\varepsilon}}^{\text{acc}} = \boldsymbol{m} \cdot \hat{\varepsilon}^{\text{acc}} = \boldsymbol{m} \cdot f_{\text{apml}} \hat{f}_N f_e f_p f_Y f_\pi \qquad (2)$$

These empirical factors (f_{apml}; $\hat{f}_N$; f_e; f_p; f_Y; f_π), see Table 1, considering the influence of the strain amplitude, the void ratio, the mean effective pressure, the stress ratio, polarisation changes, and the historiotropy on the accumulation effects. The HCA model is calibrated on numerous high cyclic tests (Wichtmann, 2016).

Table 1. Functions and parameters of the HCA model (Niemunis et al., 2005; Wichtmann, 2016)

Function	Parameters
$f_{\text{ampl}} = \min\left\{\left(\frac{\varepsilon^{\text{ampl}}}{10^{-4}}\right)^{C_{\text{ampl}}}; 10^{C_{\text{ampl}}}\right\}$	C_{ampl}
$\hat{f}_N = \hat{f}_A + \hat{f}_B$	
$\hat{f}_A = C_{N1} C_{N2} \exp\left[-\frac{g^A}{C_{N1} f_{\text{ampl}}}\right]$	C_{N1} C_{N2} C_{N3}
$\hat{f}_B = C_{N1} C_{N3}$	
$f_e = \frac{(C_e - e)^2}{1+e} \frac{1 + e_{\max}}{(C_e - e_{\max})^2}$	C_e
$f_p = \exp\left[-C_p \left(\frac{p^{av}}{100\ \text{kPa}} - 1\right)\right]$	C_p
$f_Y = \exp(C_Y \bar{Y}^{av})$	C_Y
$f_\pi = 1$ (for constant polarization)	

The numerical implementation of this constitutive theory combines the conventional implicit with the explicit simulation approach in separate modes of operations, see Figure 2. In the explicit calculation mode, only the accumulation trend is considered. The scalar strain amplitude $\varepsilon^{\text{ampl}}$ required for Equation (2) results from the multidimensional strain path, which is recorded in the implicit calculation mode (Niemunis et al., 2005). For the present work, the implicit calculation steps were performed using the constitutive model of hypoplasticity (von Wolffersdorf, 1998) with the extension of intergranular strain (Niemunis and Herle, 1998). For hypoplasticity with intergranular strain, the incrementally nonlinear tensorial Equation (3) applies:

$$\dot{\boldsymbol{\sigma}} = M(\boldsymbol{\sigma}, \dot{\boldsymbol{\varepsilon}}, \boldsymbol{h}, e) : \dot{\boldsymbol{\varepsilon}} \qquad (3)$$

In Equation (3) the fourth-order tensor M represents a stiffness, that depends on the direction of $\dot{\boldsymbol{\varepsilon}}$, the void ratio e, and the stress state $\boldsymbol{\sigma}$. The recent history of the previous strain is stored in the intergranular strain $\boldsymbol{h}$, which causes an increased stiffness during a load reversal. Consequently, $\boldsymbol{h}$ also affects the stiffness. In the framework of the implicit calculation, $d\,\sqcup/dt = \dot{\sqcup}$ is denoted as the derivative of time. The integration of the constitutive model in this calculation period is incremental, i.e. with many small strain increments.

The parameters of Karlsruhe fine sand (KFS) have been used in the FE calculations in this paper, see Tables 2, 3, and 4. This set of parameters has already been used for various other boundary value problems (Staubach et al., 2020; Wichtmann, 2016).

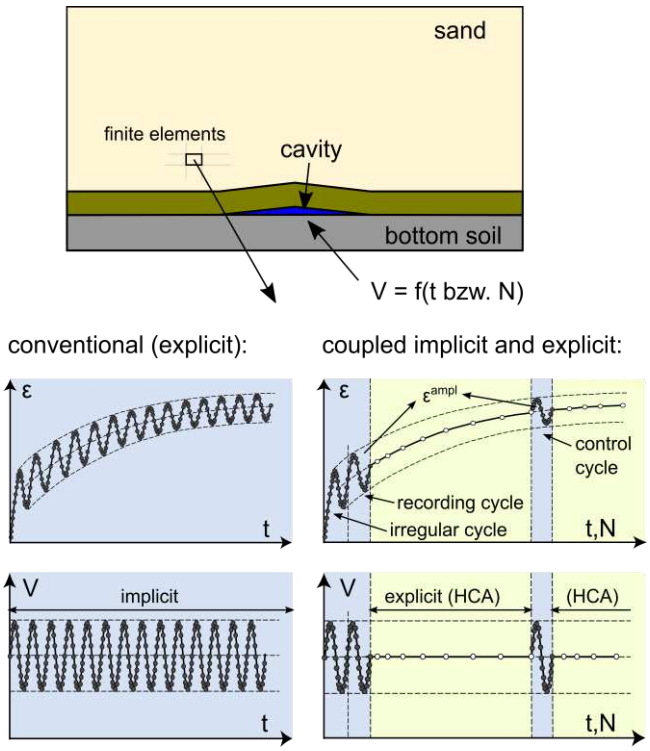

Figure 2. FE-calculation: explicit vs. coupled implicit and explicit calculation, modified from Wichtmann (2016)

Due to the large maximum mean effective pressure in the boundary value problem investigated in this work, the factor $C_p = 0.09$ is chosen. For a mean effective pressure of $p \approx 900$ kPa, $C_p = 0.09$ was experimentally confirmed by Knittel et al. (2022). Previously, $C_p = 0.23$ was proposed for a mean effective pressure of $p \approx 300$ (Wichtmann, 2016). It should be noted that the maximum effective pressure in the analysed boundary value problem ($p \approx 1500$ kPa) is still higher than the experimentally confirmed applicability limits of the HCA model.

Table 2. Parameters of hypoplasticity for KFS

φ_c	e_{io}	e_{c0}	e_{d0}	h_s	n	α	β
33.1°	1.212	1.054	0.677	4GPa	0.27	0.14	2.5

Table 3. Parameters of the intergranular strain for KFS

R	m_R	m_T	β_R	χ
10^{-4}	2.4	1.2	0.1	6.0

Table 4. Parameters of the HCA model for KFS

C_{ampl}	C_e	C_p	C_Y	C_{N1} [10^{-4}]	C_{N2}	C_{N3}
1.33	0.6	0.09	1.68	2.95	0.41	1.90

3 BOUNDARY VALUE PROBLEM

The axisymmetric boundary value problem, see Figure 3, consists of: (1) A flat circular cavity of radius $R = 25$ m located at a depth of $T = 100$ m below ground level. (2) A bottom soil layer below the cavity, which is assumed to be linear-elastic ($E = 10000$ MPa; $\nu = 0.3$). (3) A load distribution layer, which is also considered linear elastic ($E = 500$ MPa; $\nu = 0.25$). (4) The overlying sand, where the described HCA model was applied.

It is assumed that an impermeable geologic barrier located above the cavity would be required to create the cavity in the subsurface. This layer would lead to load distribution. Taking such a layer into account in the numerical model reduces discontinuities and is therefore also numerically advantageous.

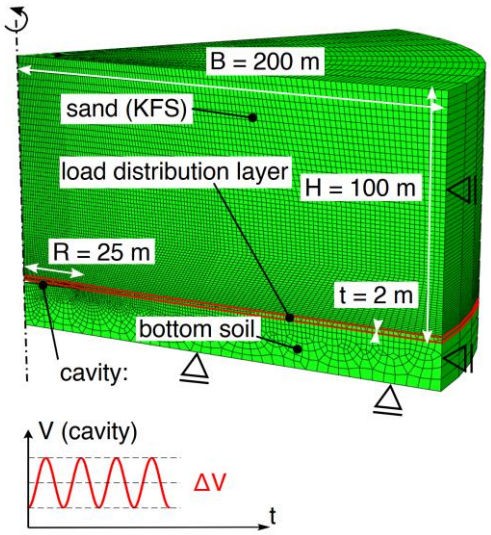

Figure 3. Investigated axisymmetric boundary value problem and boundary condition for the cavity volume

Because of the low frequency of the energy storage cycles (one cycle per day), the problem can be solved by neglecting the inertial forces (quasi-static). For the initial spatial stress distribution, dry sand of weight $\gamma = 20$ kN/m^3 is assumed. The calculations were conducted using the commercial finite element program Abaqus/Standard, which offers the possibility to implement user-defined constitutive models via subroutines. The calculations in this paper were conducted using the user-defined subroutine "umat" provided by one of the authors A. Niemunis.

Abaqus enables the modeling of fluid-filled cavities and their hydraulic coupling. For this purpose, two cavities must be defined and linked together using so-called fluid link elements. A given volume change in one of the two cavities leads to a fluid volume exchange of the incompressible fluid between the two cavities (Norlyk et al., 2020). A pressure balance between the cavities is achieved.

To minimize undesirable self-stresses within the elements in simulations with the HCA model, EAS elements or at least elements with reduced integration should be selected (Niemunis and Melikayeva, 2015). Overall 9960 two-dimensional, axisymmetric elements (CAX4R) were used.

The mechanical boundary conditions are shown in Figure 3. As an initial condition, a linear decrease in

void ratio with depth was chosen. This ensures a nearly constant initial relative density in the sand at the surface as well as at a depth of 98 m. The pressure-related relative density I_{d0} (Equation (4)) is therefore evaluated with the compression relation according to Bauer (1996) (Equation (5)). A constant void ratio in the whole model over the 100 m depth would be physically not reasonable. In the vertical direction, the initial intergranular strain was assumed to be fully mobilised. No cyclic preloading was applied, $g^A = 0$.

$$I_{d0}(p) = \frac{e_d(p) - e}{e_d(p) - e_c(p)} \approx const. \quad (4)$$

$$\frac{e_d(p)}{e_d(p=0)} = \frac{e_c(p)}{e_c(p=0)} = exp\left[-\left(\frac{3p}{h_s}\right)^n\right] \quad (5)$$

4 NUMERICAL RESULTS

In the following, the calculation results are analysed from the perspective of cumulative deformations caused by the high cyclic loading as well as from the perspective of the desired energy storage. For a better understanding of the system, the relative initial density, the lateral pressure coefficient, and the volume amplitude were varied between the calculations.

4.1 Mechanical behaviour of soil

The total settlements at the surface above the cavity, the spatial distribution of the void ratio, and the field of the mean effective pressure are discussed in the following.

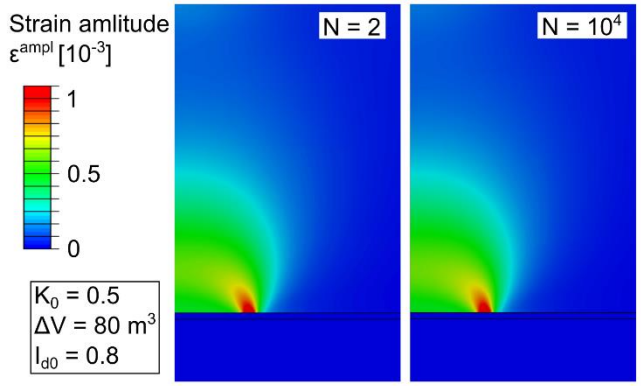

Figure 4. Strain amplitude after N = 2 and N = 10^4 cycles

Figure 4 illustrates the field of the scalar strain amplitude after $N = 2$ (first HCA mode) and $N = 10^4$ (last HCA mode) cycles. The maximum strain amplitude is concentrated above the outer edge of the cavity. The control cycles only insignificantly influence the spatial distribution of the strain amplitude.

In Figure 5, the development of the settlements with an increasing number of cycles at various points on the surface of the ground is presented. The six implicitly calculated cycles and the four HCA phases are shown. The first irregular cycle leads to large settlements. In the subsequent regular cycles, the rate of accumulation decreases with an increasing number of cycles. The greatest settlement was calculated at the symmetry axis ($R = 0$ m). The settlements of the surface of the ground decrease with increasing distance from the symmetry axis ($R = 50$ m, $R = 150$ m).

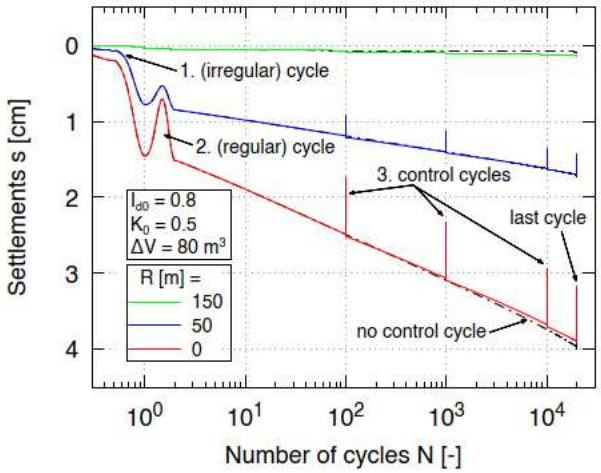

Figure 5. Settlements of the surface of the ground as a function of the number of cycles at various points

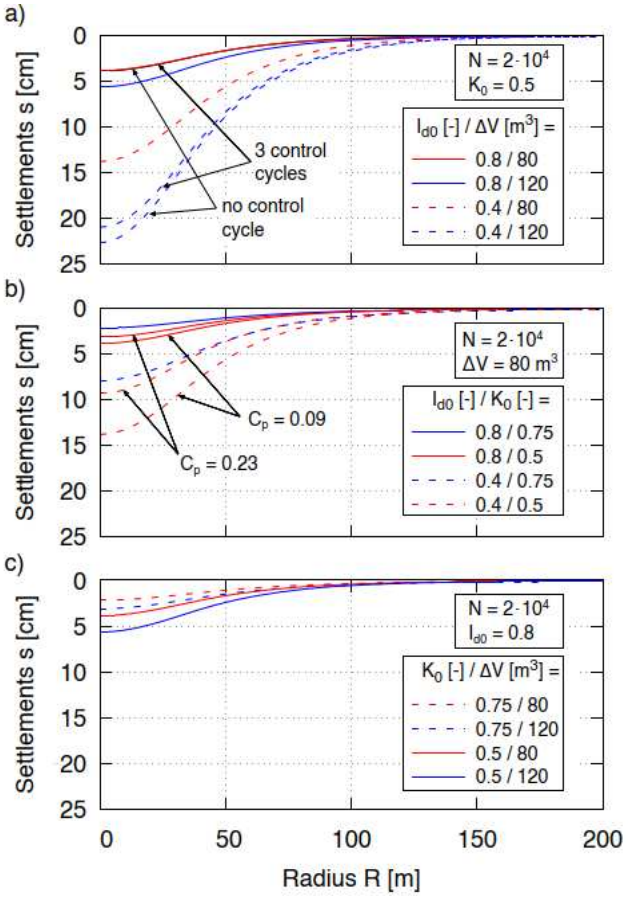

Figure 6. Settlements of the surface of the ground after $N = 2 \cdot 10^4$ cycles for (a) a constant lateral pressure coefficient, (b) a constant volume amplitude, (c) a constant initial relative density

The settlements after $N = 2 \cdot 10^4$ cycles are shown in Figure 6 for different variants. As expected, decreasing the initial density and the lateral pressure coefficient leads to an increase in the settlements. Additionally, the settlements increase with a larger inflated volume amplitude.

Figure 6(a) and Figure 5 are showing that in the given boundary value problem, the influence of control cycles, in which the strain amplitude is updated, is of minor importance. As Figure 4 shows, the strain amplitude changes only slightly due to the control cycles. This is consistent with the observations of quasi-static problems of the deformations of monopile foundations for wind turbines in saturated ideally drained sand (Staubach et al., 2020). If not otherwise specified, the calculations were performed using three control cycles.

As shown in Figure 6(b), the parameter C_p has a significant impact on the calculated settlements. A reduction of C_p leads to larger settlements. As described, experiments have confirmed $C_p = 0.23$ for $p = 300$ kPa and $C_p = 0.09$ for $p = 900$ kPa. For the investigated boundary value problem with $p \approx 1500$ kPa, a lower C_p value and consequently larger settlements could be expected.

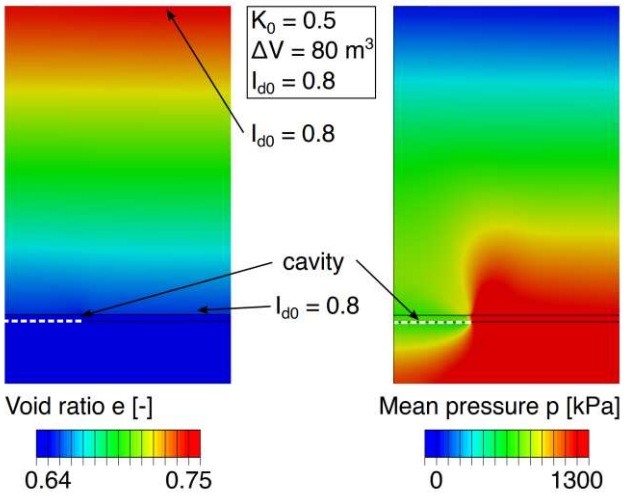

Figure 7. Void ratio and mean effective pressure after $N = 2 \cdot 10^4$ cycles

Figure 7 shows the spatial distribution of the void ratio and the mean effective pressure after $N = 2 \cdot 10^4$ cycles. The mean effective pressure in the region above the cavity is significantly reduced as a result of the densification and the relaxation due to cyclic loading. Although, the field of the void ratio is only slightly affected. According to Equation (4-5), the pressure-related density increases slightly. This is a result of the decrease in mean effective pressure (relaxation), while the void ratio almost remains constant. It should also be noted that no instabilities can be seen throughout the calculations. This is due to the minimal uplift of the soil mass in comparison to the overburden height.

Previous simulations with a greater uplift in relation to the overburden height result in significant soil deformation and shear band formations. This leads to a reduction of the overburden height and causes instabilities of the overall system (Norlyk et al., 2020; Stutz et al., 2020). These effects do not occur in the novel UPHES studied in this work.

4.2 Energy considerations

For the energy loss during a single charging and discharging of the cavity, applies

$$\Delta E = \underbrace{\int_{V_0}^{V_1} p dV}_{E_{\text{in}}} - \underbrace{\int_{V_1}^{V_0} p dV}_{E_{\text{out}}} \tag{6}$$

where p is the fluid pressure inside the cavity and V is the volume of the cavity. The limits of the integration V_0 and V_1 represent the minimum and maximum fluid volume in the cavity during energy storage. The energy efficiency of the soil mechanical system equals

$$\omega = \frac{E_{\text{out}}}{E_{\text{in}}} \tag{7}$$

wherein the quantities of energy E_{in} and E_{out} can be determined according to Equation (6). The soil-mechanical system in situ is affected by the energy losses calculated in this work. Additional energy losses in a real UPHES system are in the order of a typical pumped hydroelectric energy storage system (20%) (Blakers et al., 2021).

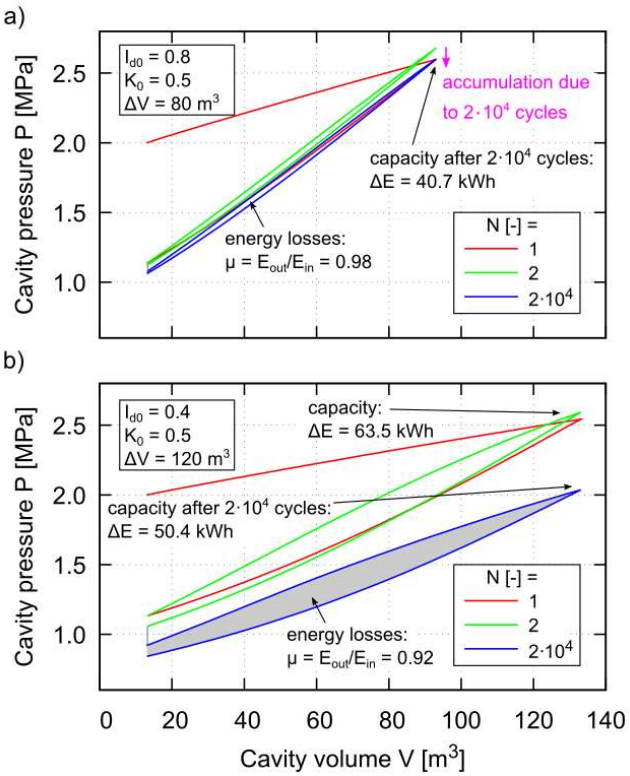

Figure 8. Energy storage: (a) large efficiency and small capacity, (b) increased capacity and reduced efficiency

Figure 8 shows the cavity pressure-volume curves for two distinct cases of the investigated variants. Initially, the injected volume causes a significant increase in cavity pressure. Once the cavity is discharged, the pressure drops again. The initial (irregular) cycle is very different from the succeeding regular cycles and won't be discussed further.

Figure 8(a) shows an estimated energy storage capacity of 40.7 kWh with 98% efficiency. Because of the minor accumulation effects, the energy storage capacity and efficiency remain nearly constant. This variation causes settlements of around 4 cm at the surface. When the initial relative density is lower and the volume amplitude is increased, see Figure 8(b), the capacity for the initial storage cycles is about 63.5 kWh. This variation, however, exhibits much higher energy losses per cycle and cumulative effects. This leads to a 20% reduction in the energy storage capacity and a 92% efficiency after $N = 2 \cdot 10^4$ cycles. This variation also caused total settlements on the ground of about 21 cm.

5 CONCLUSIONS

In this paper, the HCA model was used to investigate a novel UPHES system with a significant overburden height and low volume amplitudes. To the authors' knowledge, it's the first time that such investigations have been carried out. An axisymmetric finite element model with a fluid cavity link of Abaqus/Standard was used.

The HCA model was used to examine the trend of the accumulation effects to study the long-term behaviour as a result of hundreds of cycles. Despite the rather simple numerical model, the limitations in the constitutive models, and the assumptions made, these calculations have the potential to advance the design of geotechnical gravitative energy storage systems. The investigations predicted settlements of 2.5 to 23 cm depending on the initial density, initial stress condition, and cavity volume amplitude. At low relative densities, small lateral pressure coefficients, and high amplitudes, accumulation effects are considerable. Pressure and volume analysis reveals good capacity and efficiency of the system.

Nevertheless, the UPHS system under investigation has a 50 kWh capacity and up to 98% efficiency due to the soil mechanical dissipation. In the future, further investigations on the underground pumped hydroelectric storage (UPHES) system will be carried out based on the presented results.

6 ACKNOWLEDGMENTS

The author thanks P. Staubach and V. Osinov for the discussions about the HCA model and its implementation.

7 REFERENCES

Bauer, E. 1996. Calibration of a comprehensive hypoplastic model for granular materials, *Soils and Foundations* **36**, 13–26.

Blakers, A., Stocks, M., Lu, B., Cheng, C. 2021. A review of pumped hydro energy storage, *Progress in Energy* **3(2)**, 022003.

Franza, A., Sørensen, K., Stutz, H.H., Pettey, A., Heron, C., Marshall, A.M. 2022. Field and centrifuge modelling of a pumped underground hydroelectric energy storage system in sand. *Proceedings, 10th International Conference on Physical Modelling in Geotechnics (ICPMG),* KAIST, Daejeon, Korea.

Knittel, L., Wappler, A., Niemunis, A., Stutz, H.H. 2022. The high-cyclic model for sand tested beyond the usual ranges of application, *Acta Geotechnica* (submitted).

Niemunis, A., Herle, I. 1997. Hypoplastic model for cohesionless soils with elastic strain range, *Mechanics of cohesive-frictional materials* **2**, 279-299.

Niemunis, A., Wichtmann, T., Triantafyllidis, T. 2005. A high-cycle accumulation model for sand, *Computers and Geotechnics* **32**, 245–263.

Niemunis, A., Melikayeva, I. 2015. Improved integration of high-cycle accumulated strain using hierarchical and EAS finite elements. *Holistic Simulation of Geotechnical Installation Processes. Numerical and Physical Modelling.* Eds: Triantafyllidis, T., 181-205. Springer.

Norlyk, P., Sørensen, K., Vabbersgaard Andersen, L., Sørensen, K.K., Stutz, H.H. 2020. Holistic simulation of a subsurface inflatable geotechnical energy storage system using fluid cavity elements, *Computers and Geotechnics* **127**, 1–11.

Olsen, J., Paasch, K., Lassen,B., Veje, C.T. 2015. A new principle for underground pumped hydroelectric storage, *Journal of Energy Storage* **2**, 54–63.

Osinov, V.A. 2017. Some Aspects of the Boundary Value Problems for the Cyclic Deformation of Soil. *Holistic Simulation of Geotechnical Installation Processes. Theoretical Results and Applications.* Eds: Triantafyllidis, T., 150-167. Springer.

Sørensen, K., Stutz, H.H., Brødsgaard-Raptis, P., Luxhøj, M. 2021. Conceptual physical modelling of a subsurface geomembrane energy storage system. *Proceedings, 20th International Conference on Soil Mechanics and Geotechnical Engineering*. Sydney 2021.

Staubach, P. Wichtmann, T. 2020. Long-term deformations of monopile foundations for offshore wind turbines studied with a high-cycle accumulation model, *Computers & Geotechnics* **124**, 1–21.

Stutz, H.H., Norlyk, P., Sørensen, K., Vabbersgaard Andersen, L., Sørensen, K.K., Clausen J. 2020. Finite element modelling of an energy-geomembrane underground pumped hydroelectric energy storage system. *E3S Web of Conferences* **205**.

Wichtmann, T. 2016. *Soil behaviour under cyclic loading – experimental observations, constitutive description and applications*, Habilitation thesis, Publications of the Institute of Soil Mechanics and Rock Mechanics, Karlsruhe Institute of Technology, Issue No. 181.

von Wolffersdorff, P.-A. 1996. A hypoplastic relation for granular materials with a predefined limit state surface, *Mechanics of cohesive-frictional materials* **1**, 251-271.